RAPID COMMUNICATIONS

PHYSICAL REVIEW B VOLUME 52, NUMBER 18 1 NOVEMBER 1995-II

Neutron-diffraction study of the magnetic-field-induced metal-insulator transition in $Pr_{0.7}Ca_{0.3}MnO_3$

H. Yoshizawa and H. Kawano*
Neutron Scattering Laboratory, Institute for Solid State Physics, University of Tokyo, Shirakata 106-1, Tokai, Ibaraki 319-11, Japan

Y. Tomioka
Joint Research Center for Atom Technology (JRCAT), Tsukuba 305, Japan

Y. Tokura
Department of Applied Physics, University of Tokyo, Tokyo 113, Japan
and Joint Research Center for Atom Technology (JRCAT), Tsukuba 305, Japan
(Received 1 September 1995)

Without a magnetic field $Pr_{0.7}Ca_{0.3}MnO_3$ exhibits three phase transitions: a change of the lattice symmetry at $T_B=200$ K, an antiferromagnetic ordering at $T_N=140$ K, and a canted antiferromagnetism at $T_{CA}=110$ K. Although the resistivity of $Pr_{1-x}Ca_xMnO_3$ shows insulating behavior at zero field, it exhibits an insulator-metal (I-M) transition at around 4.0 T at 5 K. An applied field enforces a ferromagnetic spin alignment and drives $Pr_{1-x}Ca_xMnO_3$ into the metallic state by actuating the double-exchange mechanism and destroying the charge ordering. This I-M transition at 5 K is accompanied by a large hysteresis.

Recently, a large negative magnetoresistance has been discovered in distorted perovskite manganese oxides.[1–8] As is well known, perovskite manganese oxides such as $La_{1-x}Sr_xMnO_3$ and $La_{1-x}Ca_xMnO_3$ transform from an antiferromagnetic insulator to a ferromagnetic metal as a function of dopant concentration.[9–11] This phenomenon has been known as mediated by a double exchange interaction.[12–14] One of the distorted perovskite oxides, a $Pr_{1-x}Ca_xMnO_3$ system, however, remains insulating against Ca doping.[15–17] Its resistivity shows insulating behavior over the whole Ca ion concentration. This is partly because the charge-transport in $Pr_{1-x}Ca_xMnO_3$ is amenable to the charge ordering of Mn^{3+} and Mn^{4+} near $x\sim0.5$. Similar charge-ordering phenomena in other distorted perovskite manganese oxides have been reported in $La_{1-x}Ca_xMnO_3$ ($x\approx1/2$),[10] $Pr_{1/2}Sr_{1/2}MnO_3$,[18,19] and $Nd_{1/2}Sr_{1/2}MnO_3$.[20] In general, the cations with smaller ionic radii in (R,A) sites of $R_{1-x}A_xMnO_3$ cause a larger alternating tilting of MnO_6 octahedra in a pseudoperovskite $GdFeO_3$-type structure, and leads to a distortion-dependent reduction of a one-electron bandwidth through a tolerance factor.[21] Consequently, a small one-electron bandwidth in aforementioned manganese oxides causes a charge-ordered state, and stabilizes simultaneously an antiferromagnetic spin structure. Recently, Tomioka *et al.* have reported that an applied field can cause a melting of such charge ordering and then results in the insulator-metal (I-M) transition on the H-T phase diagram in $Pr_{1-x}Ca_xMnO_3$ (Ref. 22) as well as $Pr_{1/2}Sr_{1/2}MnO_3$.[19] A field of a few tesla can also cause a lattice symmetry switching in a related compound $La_{1-x}Sr_xMnO_3$ ($x=0.17$).[23] Such recent research activity has shed light on a variety of charge-spin coupled properties on distorted perovskite manganese oxides, opening a possibility of controlling magnetic and transport properties and even a lattice structure by an external magnetic field. In the present paper, we shall study magnetic and structural aspects of the I-M transition in $Pr_{0.7}Ca_{0.3}MnO_3$ by neutron-diffraction technique.

Powder samples were prepared by calcining the mixture of prescribed amount of Pr_6O_{11}, $CaCO_3$, and Mn_3O_4 in air at 1200 °C for a few times, and pressed into rods. Single-crystal samples were melt grown by a floating-zone method in gas of 100% O_2 with a traveling speed of 3–5 mm/h. The Ca composition x was examined by the electron-probe microanalysis, giving an accuracy of x being ±0.01. Neutron-diffraction measurements were performed on a triple-axis spectrometer GPTAS installed at a beamtube 4G in the JRR-3M of JAERI, Tokai. For most of the measurements, incident neutron momentum $k_i=2.57$ Å^{-1} with a combination of 40′-40′-40′ collimators was utilized, while for part of the measurements the spectrometer was operated with $k_i=3.825$ Å^{-1} and a combination of 20′-20′-20′ collimators in order to access a wider range of the momentum space. A crystal of $Pr_{0.7}Ca_{0.3}MnO_3$ belongs to the space group $Pbnm$, and the measurements were performed with the $(h,k,0)$ scattering plane with a magnetic field parallel to the [001] axis.

The crystal and magnetic structures of the $Pr_{1-x}Ca_xMnO_3$ system were studied in detail by Jirak *et al.*[17] For the $x=0.3$ sample, it shows a canted ferromagnetic structure accompanied with antiferromagnetic (AF) components of a so-called pseudo CE-type AF structure as shown in Fig. 1. Furthermore, the charge ordering of Mn^{3+} and Mn^{4+} ions takes place simultaneously with a lattice distortion described as buckling, where MnO_6 octahedra show alternating tilting and cause a doubling of the periodicity of the lattice along the [010] direction. According to Jirak *et al.*,[17] intense superlattice reflections were observed at (2, 1.5, 0) and (2, 2.5, 0) for powder sample measurements.

The temperature dependences measured at selected Bragg reflections are illustrated in Fig. 2. The behavior of the fer-

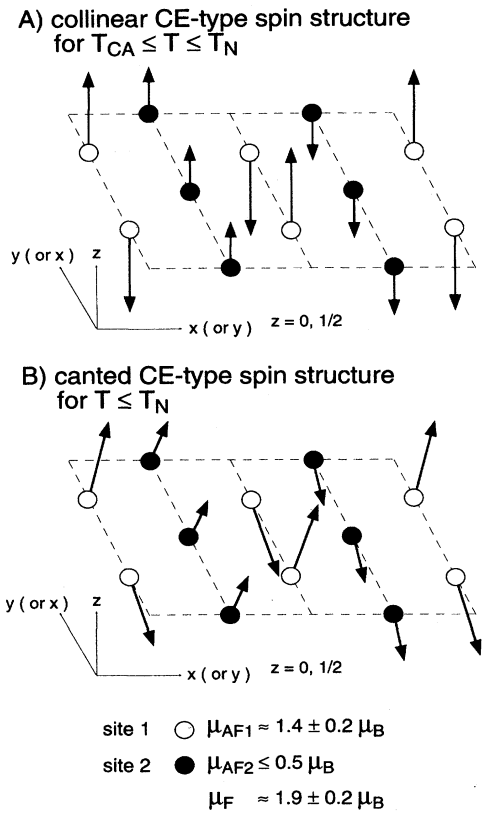

FIG. 1. The schematic spin structure of the pseudo-CE-type antiferromagnetic structure (a) for the collinear intermediate phase and (b) for the canted low-temperature phase. Lines of open circles (site 1) and closed circles (site 2) may appear either along the x direction or along the y direction due to domain.

romagnetic (F) long-range order (LRO) can be studied by observing the Bragg reflections at $Q=(h,k,0)$ with h,k *integer* and $h+k=$*even*. With decreasing temperature, the intensity at (1, 1, 0) increases gradually below $T_B \sim 200$ K, reflecting the onset of the charge ordering as well as the buckling in the $Pr_{0.7}Ca_{0.3}MnO_3$ sample, and then shows a steep rise below $T_{CA} \sim 110$ K. The diffuse scattering observed at (1, 0.94, 0) also exhibits a clear cusp at T_{CA}. These features indicate the clear phase transition and the onset of the F component at T_{CA}. Second, behavior of the CE-type antiferromagnetic (AF) LRO can be studied at $Q=$(*half integer, half integer,* 0) and (*integer, half integer,* 0). The intensity of both (0.5, 0.5, 0) and (1, 0.5, 0) increases steeply at $T_N \sim 140$ K and then continues to grow below $T_{CA} \sim 110$ K. As illustrated in Fig. 1, the $Pr_{0.7}Ca_{0.3}MnO_3$ sample shows a collinear AF order below $T_N \sim 140$ K and changes into a pseudo-CE-type canted AF order at $T_{CA} \sim 110$ K. From the intensity analysis, the AF moments for the pseudo-CE-type structure at 5 K was determined to be $\mu_{AF1} \sim 1.4 \pm 0.2 \mu_B$ for the site 1 in Fig. 1 and $\mu_{AF2} < 0.5 \mu_B$ for the site 2, respectively. Only the upper limit of the moment was evaluated for the site 2 due to uncertainties caused from the influence of other domains. The ferromagnetic moment μ_F was determined to be $\mu_F \sim 1.9 \pm 0.2 \mu_B$, being in good agreement with the value evaluated from the bulk magnetization measurements,

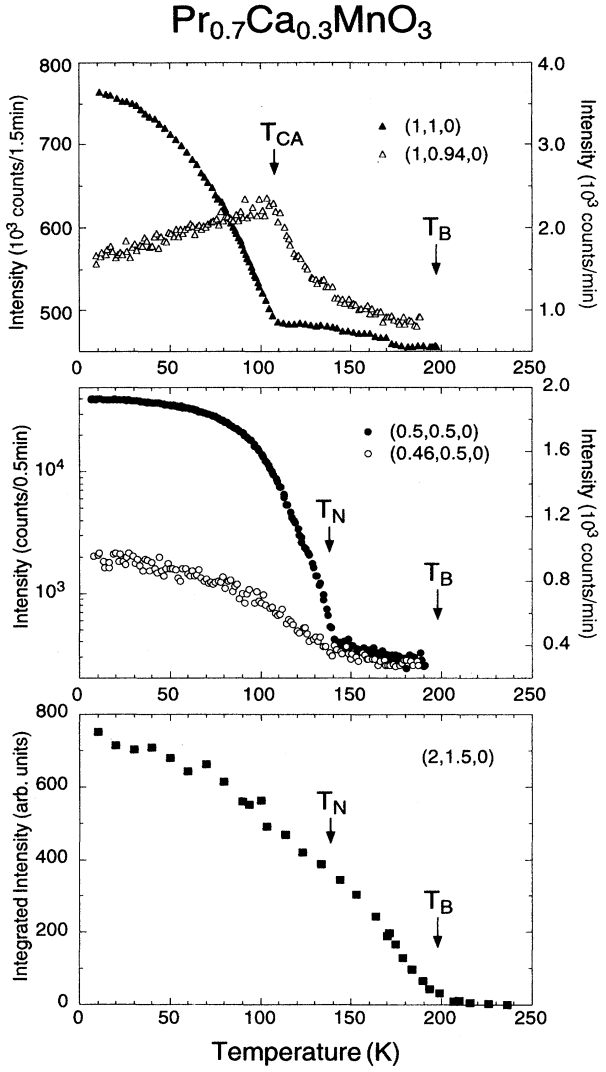

FIG. 2. The temperature dependence of various representative Bragg reflections. The onset of the buckling and the charge ordering is denoted by T_B, the collinear CE-type antiferromagnetism by T_N, and the canted ferromagnetism by T_{CA}, respectively. Open marks in panels of (1, 1, 0) and (0.5, 0.5, 0) are the temperature dependences of the diffuse scattering observed at the respective offset positions, and the scales of their intensity are depicted on the right ordinates.

$\mu_F = 1.7 \mu_B$.[24] The total moment $\mu_{tot} \sim 2.36 \mu_B$ is rather small from the spin only value $3.7 \mu_B$ expected from Mn^{3+} and Mn^{4+} ions. As described in the following, this is because part of the spins does not contribute to the LRO, but forms a spin-glass-like state.

The lattice distortion due to the charge ordering and the buckling of MnO_6 octahedra can be studied at $Q=$(*integer, half integer,* 0). At (2, 1.5, 0) where the magnetic scattering is relatively weak, a superlattice reflection due to the buckling of the lattice is clearly observed below $T_B \sim 200$ K, indicating a formation of the charge ordering. Below $T_N \sim 140$ K, there can be a weak contribution of the AF magnetic Bragg scattering.

According to the bulk magnetization measurements on

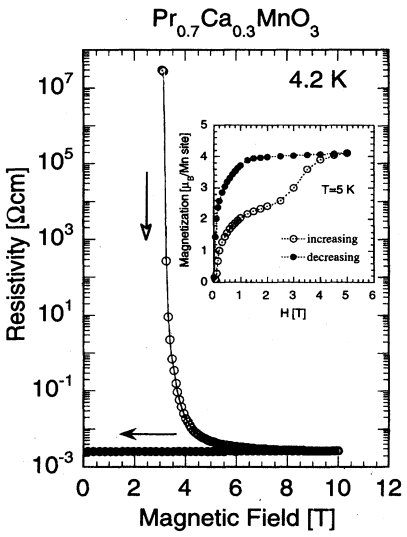

FIG. 3. The field dependence of resistivity at 4.2 K. (Inset) The field dependence of the magnetization observed at 5.0 K.

$Pr_{0.7}Ca_{0.3}MnO_3$,[24] spontaneous magnetization appears below $T_{CA}\sim 110$ K, and the irreversibility was observed below 80 K between the zero-field-cooled (ZFC) magnetization and the field-cooled (FC) magnetization, suggesting the spin-glass state in $Pr_{0.7}Ca_{0.3}MnO_3$. Corresponding to the irreversibility of magnetization, magnetic diffuse scattering was observed around the AF Bragg reflection (0.5, 0.5, 0). To examine the temperature dependence of the diffuse scattering, we measured the temperature dependence of the intensity at $Q=(0.46,0.5,0)$ which is well outside the influence of the Bragg reflection, and the result is plotted in the panel of (0.5, 0.5, 0) in Fig. 2. The diffuse scattering observed at $Q=(1,0.94,0)$ near the ferromagnetic Bragg reflection exhibits a cusp at T_{CA}, and decreases linearly below T_{CA}, indicating that a major part of the intensity is dominated by the transverse susceptibility, namely, spin-wave scattering. By contrast, the diffuse intensity observed at $Q=(0.46,0.5,0)$ increases monotonically. These results indicate that there is an intense diffuse scattering due to frozen spin disorder at low temperatures.

For $Pr_{0.7}Ca_{0.3}MnO_3$, the concentration x of Mn^{3+} ions does not take a commensurate value such as $x=1/4$, 1/3, and 1/2. The observed magnetic structure in the present study is that of the commensurate value $x=1/2$, i.e., the pseudo-CE-type AF $2\sqrt{2}\times 2\sqrt{2}$ structure as was reported in an early study.[17] Therefore, when the charge ordering is formed based on the CE-type configuration, excess Mn^{3+} ions are randomly interspersed over the Mn^{4+} sites, and then introduce randomness of the exchange interactions when they are localized. As a result, an average moment on a site 2 in Fig. 1 is strongly reduced, and the spin-glass-like behavior appears at low temperatures.

According to the resistivity and bulk magnetization measurements on $Pr_{0.7}Ca_{0.3}MnO_3$, the I-M transition takes place at $\sim$4.0 T at low temperatures.[24] The field dependence of resistivity observed at 4.2 K and the magnetization at 5.0 K are depicted in Fig. 3. Both measurements were performed after the sample was cooled to a prescribed temperature under zero field. In the first field-increasing run for 4.2 K measurements, the resistivity starts dropping around 3.0 T from an insulating value (larger than 10^7 Ω cm) and reaches to a metallic value of order of 10^{-3} Ω cm. In the subsequent field-decreasing run, the resistivity remains unchanged with its metallic value down to 0.0 T.

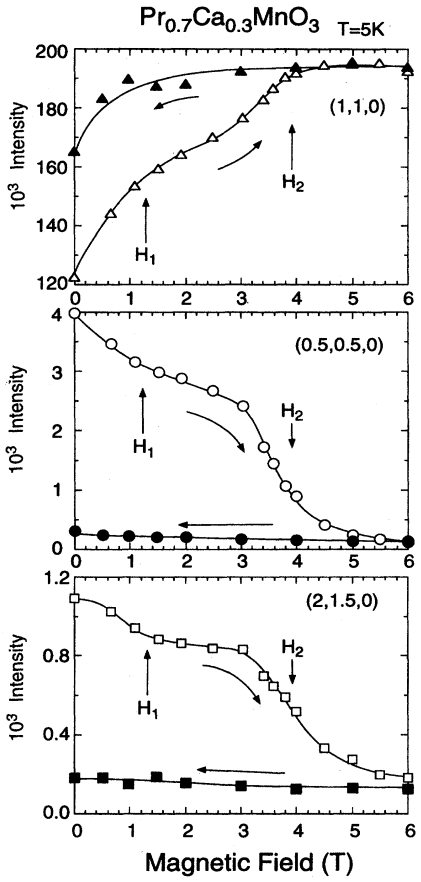

FIG. 4. The field dependences of three types of Bragg reflections at 5 K. H_1 and H_2 denote two anomalies observed in the field-increasing run.

In the inset of Fig. 3 is shown the field dependence of the magnetization observed at 5.0 K. Although the measurement temperature is not exactly identical with that of resistivity, the correlation between resistivity and the magnetization is clear. The virgin magnetization curve exhibits two shoulders, one at $H\sim 1$ T and the other at $H\sim 3.5$ T, then saturates for $H\gtrsim 4$ T, while in the subsequent field-decreasing process and the second run, it follows the same ferromagnetic curve. Clearly, when the magnetization is saturated, the system shows metallic resistivity. In order to further study the relationship between the resistivity and the magnetism, the magnetic behavior was studied in detail by measuring the integrated intensity of three Bragg reflections through a $\theta-2\theta$ scan.

Figure 4 shows the field dependences of the integrated intensity for the F, AF, and B components observed at 5 K, respectively. All the measurements were performed after the sample was cooled to a prescribed temperature under zero field. In the field-increasing run at 5 K, two anomalies were

observed as indicated by H_1 and H_2. For the F component observed at (1, 1, 0), one can see the first shoulder at $H \sim H_1$. On the other hand, for the AF components at (0.5, 0.5, 0) as well as the B component at (2, 1.5, 0), the intensity quickly decreases till H_1, and then levels off. By inspecting profiles, we found that the diffuse scattering also decreased rapidly. These changes suggest that the spins contributing to the spin-glass component are aligned towards the field direction. Since the resistivity for $H < 3.0$ T has a large insulating value, the change of the spin-glass component caused by an applied field is not responsible for the I-M transition. This constitutes the interpretation of the first shoulder in the magnetization curve.

Now we move to the interpretation of the second shoulder. A distinct metamagnetic anomaly was also observed by neutron scattering at $H \sim H_2$ (4.0 T). The intensity of (1, 1, 0) showed a steplike increase, whereas those of (0.5, 0.5, 0) and (2, 1.5, 0) dropped rapidly and almost vanished.

This behavior indicates that AF components go through a spin-flip transition near H_2, and the system becomes ferromagnetic. This anomaly exactly corresponds to the second shoulder of the magnetization curve and to a steep decrease in resistivity. Therefore, we see that an applied field forces alignment of the AF components towards the field direction, and then actuates the double exchange mechanism, giving rise to the metallic state. At the same time, the intensity of (2, 1.5, 0) shows a substantial decrease, indicating that the I-M transition releases most of the lattice distortion by melting the charge ordering. In the field-decreasing process, the resistivity retains its metallic value. Corresponding behavior was observed for all three Bragg reflections. The integrated intensity of each component retains its value at 6.0 T except for a small decrease of the (1, 1, 0) intensity below 0.5 T, at which part of the system recovers a spin-glass-like disorder. The hysteretic behavior indicates a strong coupling between spins and charges.

For the measurements of the isothermal field dependence shown in Fig. 4, the intensity of the buckling component (2, 1.5, 0) did not vanish completely in the metallic phase. Since the buckling component satisfies one of the reflection conditions for the CE-type AF structure, we evaluated the magnetic contribution at (2, 1.5, 0) by assuming that the intensity observed at (1, 0.5, 0) is purely magnetic, and found that the dominant contribution to the intensity at $Q = (2, 1.5, 0)$ comes from the buckling component. Therefore, we can conclude that a finite buckling distortion persists in the metallic phase of the $Pr_{0.7}Ca_{0.3}MnO_3$ sample. A possible origin of this scattering is the inhomogeniety of the sample studied in the neutron-diffraction measurements. As is well known, a small oxygen deficiency can cause an important change of transport as well as magnetic behavior in perovskite transition-metal oxides.[25]

In summary, we have demonstrated that for the $Pr_{0.7}Ca_{0.3}MnO_3$ sample, there is excellent correspondence between the I-M transition found in the resistivity and the change of the spin structure observed by neutron-diffraction experiments. At 5 K, the $Pr_{0.7}Ca_{0.3}MnO_3$ sample transforms to a ferromagnetic metallic state near H_2 ($\sim$4.0 T) through the metamagnetic transition. When the field is subsequently decreased, it shows a pronounced hysteresis, retaining a ferromagnetic metallic state down to 0.0 T. Very recently, it has been suggested that these I-M transitions can be viewed as a melting of the charge ordering. In fact, we have observed a drastic suppression of the superlattice intensity at (2, 1.5, 0). These results indicate that the I-M transition in the $Pr_{1-x}Ca_xMnO_3$ system takes place under the environment of the strong spin-charge coupling.

The present study was supported in part by a Grant-In-Aid for Scientific Research from the Ministry of Education, Science and Culture, Japan, and by the New Energy and Industrial Technology Development Organization (NEDO) of Japan.

*Present address: (RIKEN), Wako, Saitama 351-01, Japan.

[1] R. M. Kusters, D. A. Singleton, D. A. Keen, R. McFreevy, and W. Hayes, Physica B **155**, 362 (1989).
[2] K. Chabara, T. Ohno, M. Kasai, and Y. Kozono, Appl. Phys. Lett. **63**, 1990 (1993).
[3] R. von Helmont, J. Wecker, B. Holzapfel, L. Schultz, and K. Samwer, Phys. Rev. Lett. **71**, 2331 (1993).
[4] S. Jin, Th. H. Tiefel, M. McCormack, R. A. Fastnacht, R. Ramesh, and L. H. Chen, Science **264**, 413 (1994).
[5] H. L. Ju, C. Dwon, R. L. Greene, and T. Venkatesan, Appl. Phys. Lett. **65**, 2108 (1994).
[6] M. McCormack, S. Jin, T. H. Tiefel, R. M. Fleming, and Julia M. Phillips, Appl. Phys. Lett. **64**, 3045 (1994).
[7] Y. Tokura, A. Urushibara, Y. Moritomo, T. Arima, A. Asamitsu, G. Kido, and N. Furukawa, J. Phys. Soc. Jpn. **63**, 3931 (1994).
[8] A. Urushibara, Y. Moritomo, T. Arima, A. Asamitsu, G. Kido, and Y. Tokura, Phys. Rev. B **51**, 14 103 (1995).
[9] G. H. Jonker and J. H. van Santen, Physica **16**, 337 (1950).
[10] E. O. Wollan and W. C. Koehler, Phys. Rev. **100**, 545 (1955).
[11] G. H. Jonker, Physica **22**, 707 (1956).
[12] C. Zener, Phys. Rev. **82**, 403 (1951).
[13] P. W. Anderson and H. Hasegawa, Phys. Rev. **100**, 675 (1955).
[14] P.-G. de Gennes, Phys. Rev. **118**, 141 (1960).
[15] Z. Jirak, S. Krupicka, V. Nekvasil, E. Pollert, G. Villeneuve, and F. Zounova, J. Magn. Magn. Mater. **15-18**, 519 (1980).
[16] E. Pollert, S. Krupicka, and E. Kuzmicova, J. Phys. Chem. Solids **43**, 1137 (1982).
[17] Z. Jirak, S. Krupicka, Z. Simsa, M. Dlouha, and S. Vratislav, J. Magn. Magn. Mater. **53**, 153 (1985).
[18] K. Knizek, Z. Jirak, E. Pollert, F. Zounova, and S. Vratislav, J. Solid State Chem. **100**, 292 (1992).
[19] Y. Tomioka, A. Asamitsu, Y. Moritomo, H. Kuwahara, and Y. Tokura, Phys. Rev. Lett. **74**, 5108 (1995).
[20] H. Kuwahara, Y. Tomioka, A. Asamitsu, Y. Moritomo, and Y. Tokura (unpublished).
[21] J. B. Torrance, P. Laccore, A. I. Nazzal, E. J. Ansaldo, and CH. Niedermayer, Phys. Rev. B **45**, 8209 (1992).
[22] Y. Tomioka, A. Asamitsu, H. Kuwahara, Y. Moritomo, and Y. Tokura (unpublished).
[23] A. Asamitsu, Y. Moritomo, Y. Tomioka, T. Arima, and Y. Tokura, Nature (London) **373**, 407 (1995).
[24] Y. Tomioka, A. Asamitsu, Y. Moritomo, and Y. Tokura, J. Phys. Soc. Jpn. (to be published).
[25] Y. Okada, T. Arima, Y. Tokura, C. Murayama, and N. Mori, Phys. Rev. B **48**, 9677 (1993).